Thermal Neutron Capture Cross Section Measurements of ^{243}Am and ^{242}Pu using the new Mini-INCA α- and γ-spectroscopy station

F. Marie, A. Letourneau *, G. Fioni, O. Déruelle, Ch. Veyssière

DSM/DAPNIA, CEA-Saclay, 91191 Gif sur Yvette, FRANCE

H. Faust, P. Mutti

Institut Laue-Langevin, 38000 Grenoble, FRANCE

I. AlMahamid, B. Muhammad

Lawrence Berkeley National Lab., ESH Division, Berkeley, CA 94720, USA

Abstract

In the framework of the Mini-INCA project, dedicated to the study of Minor Actinide transmutation process in high neutron fluxes, an α- and γ-spectroscopy station has been developed and installed at the High Flux Reactor of the Laue-Langevin Institut. This set-up allows short irradiations as well as long irradiations in a high quasi-thermal neutron flux and post-irradiation spectroscopy analysis. It is well suited to measure precisely, in reference to ^{59}Co cross section, neutron capture cross sections, for all the Actinides, in the thermal energy region. The first measurements using this set-up were done on ^{243}Am and ^{242}Pu isotopes. Cross section values, at $E_n = 0.025\ eV$, were found to be $(81.8 \pm 3.6)\ b$ for ^{243}Am and $(22.5 \pm 1.1)\ b$ for ^{242}Pu. These values differ from evaluated data libraries by a factor of 9 and 17%, respectively, but are compatible with the most recent measurements, validating by the way the experimental apparatus.

Key words: Neutron, cross section, Am-243, Pu-242, spectroscopy, nuclear waste, transmutation
PACS: 25.40.Lw, 28.41.Kw, 29.30.Ep, 29.30.Kv

* Corresponding author: tel. +33 1 69 08 76 01, fax. +33 1 69 08 75 84
Email address: aletourneau@cea.fr (A. Letourneau).

Introduction

One of the crucial challenges for the nuclear industry in this century is the capability to reduce and to manage the mass inventory and the radio-toxicity of nuclear wastes coming from spent fuel of nuclear power plants. One of the field of research presently under investigation for high level activities and long-lived nuclear wastes by the scientific community is the transmutation of long-lived isotopes into shorter lived or stable ones. The incineration of nuclear wastes requires not only innovative technological solutions, necessary to built systems providing intense neutron fluxes ($> 10^{15}\ n/cm^2/s$), but also a reliable set of nuclear data. Accurate fission cross sections are necessary to estimate the incineration potential of such systems but not only. Accurate neutron capture cross sections are also needed to follow and to predict precisely the transmutation chain. These data are needed for a wide energy range including the thermal energy region.

Due to their limited role in conventional fuel cycles, minor actinides have not been extensively studied in the past few decades. Their nuclear parameters, tabulated in the three most widely used evaluated nuclear data libraries, JEFF [1], ENDF [2] and JENDL [3], are not always known with the precision required for transmutation dedicated systems [4]. This statement is especially valid in the case of $^{242gs}Am$ for which a significant discrepancy of a factor of 20 existed between JEF-2.2 (JENDL-3.2) and ENDFB-VI libraries in the capture cross section value. A recent measurement [5] has confirmed the ENDF-BVI value and that the transmutation of ^{241}Am in an high thermal neutron flux is theoretically feasible.

In this context, and following the measurement of the $^{242gs}Am$ capture cross section [5], the mini-INCA (INcineration of Actinides) project has been created [6]. The objective of the project is to extend the field of investigations to all other minor actinides 1) which play an important role in the nuclear waste inventories for future nuclear energy production scenarios [4], and 2) for which nuclear parameters are determined with significant discrepancies between different libraries [7]. The first two isotopes examined in this project are ^{243}Am and ^{242}Pu as they contribute significantly to the mass inventory of the nuclear spent fuel and as they play a significant role in the ^{241}Am transmutation chain. Indeed, ^{243}Am and ^{242}Pu are connected to form ^{244}Cm isotope, which constitutes one of the major problem when dealing with the handling and the stocking of spent fuel. Moreover ^{244}Am isotopes have very large fission cross sections and could then participate to the incineration process of ^{241}Am. But, due to their very short lifetime, fission process is extremely disadvantaged as compare to β-decay process. In consequence, very high neutron fluxes are needed to get a significant contribution of the fission process, and thus, the economy of the incineration system strongly depends on the values of the cross

sections and their accuracy. For ^{243}Am and ^{242}Pu isotopes, discrepancies of about 4% exist on the capture cross sections between the main data libraries and larger discrepancies for experimental data.

This paper will describe the new experimental installation of the Mini-INCA project at the high flux reactor of ILL, dedicated to off-line α and γ spectroscopies of irradiated samples, and present the results obtained on the capture cross sections of ^{243}Am and ^{242}Pu. It is divided into two parts: experimental method, including a description of the experimental device, and results.

Experimental Method

The Mini-INCA set-up is located at the High Flux Reactor (HFR) of the Laue-Langevin Institut (ILL) in Grenoble [10]. It consists of two complementary irradiation facilities: H9 beam channel where activation analysis of short-time irradiated samples are performed, and V4 channel where long-time irradiations are done including on-line fission cross section measurements. In the present paper, only the H9 experimental set-up is described. It provides, as it will be detailed later, essentially thermal neutrons with an intensity of the order of $6.\ 10^{14}\ n/cm^2/s$. Thanks to such an intense neutron flux, small mass samples ($< 100\mu$g) can be used with the advantages of reducing local neutron-flux perturbations and α-particles self-absorption in the target. Moreover, the high level of thermalization available in the H9 channel results in minimizing the contribution of epithermal neutrons in the reaction rate balance for most of the isotopes as shown in [11].

Activation method

The activation method is employed to measure capture cross sections in H9. Samples are irradiated into the H9 beam channel and then automatically transferred into the "Mini-INCA" chamber where α- and γ-spectroscopy analysis are performed. The evolution of a sample in a neutron flux is given by a linear system of differential equations [8]:

$$\frac{dN}{dt} = -MN \tag{1}$$

where M is a square matrix whith diagonal elements representing the total decay rate of the isotope i and the non-diagonal elements are the transition rates from isotope j to isotope i. N is a vector giving the isotope population N_i for a given isotope i. The reaction rates M_{ij} could be written in terms of reaction cross sections (σ) and decay constant (λ):

$$M_{ij} = \begin{cases} \lambda_i + \sigma_i \phi & \forall j = i \\ -\sigma_j \phi \text{ or } \lambda_j & \forall j \neq i \end{cases} \tag{2}$$

where σ_i is the combustion (capture and fission) cross section, σ_j is the capture cross section and ϕ is the integrated flux. In general, these equations are solved numerically but for low neutron fluency they could be solved analytically. In particular, for isotopic samples and short-time irradiations, as in our experiments, where double capture could be neglected, the amount N_{X+1} of isotope $X+1$ produced from the isotope X at the end of irradiation could be expressed as [1] :

$$N_{X+1} = \frac{N_X \sigma_c(X) \phi}{\lambda_{X+1} - \sigma_c(X)\phi} \left[1 - \exp\left(-(\lambda_{X+1} - \sigma_c(X)\phi) t_{irr}\right)\right], \tag{3}$$

where N_X is the quantity of initial isotope X measured at the end of irradiation, $\sigma_c(X)$ is the capture cross section, t_{irr} is the irradiation time. If the condition $\lambda_{X+1} \ll \sigma_c(X)\phi$ is fulfilled, the capture cross section can be extracted:

$$\sigma_c(X) \simeq \frac{1}{\phi\, t_{irr}} \ln\left(1 + \frac{N_{X+1}}{N_X}\right) \tag{4}$$

Quantities N_{X+1} and N_X are deduced from the measured γ- or α-line intensities I_{X+1} and I_X, respectively, and its writes:

$$\begin{cases} N_{X+1} = \dfrac{I_{X+1}}{\lambda_{X+1}\, \Omega\epsilon} \exp\left(\lambda_{X+1}\, t\right), \\ N_X = \dfrac{I_X}{\lambda_X\, \Omega\epsilon} \exp\left(\lambda_X\, t\right) \end{cases} \tag{5}$$

where t is the time between the end of irradiation and the measurement, and $\Omega\epsilon$ is the total detection efficiency. The quantity $\phi\, t_{irr}$ is the so called neutron fluency seen by the target during the irradiation and is measured directly from the analysis of a neutron flux monitor irradiated together with the sample. In general, the $^{59}Co(n,\gamma)^{60}Co$ reaction cross section is used for the normalisation, so that the measured cross section (Eq. (4)) could be expressed as a function of the $^{59}Co(n,\gamma)^{60}Co$ cross section :

$$\sigma_c(X) \simeq \frac{N_{59}\sigma_{59}}{N_{60}} \ln\left(1 + \frac{N_{X+1}}{N_X}\right) \tag{6}$$

[1] Assuming that fission cross section of X and burn-up of $X+1$ could be neglected

where N_{59} and N_{60} are the number of atoms of ^{59}Co and ^{60}Co by the end of irradiation.

Simulation of the neutron flux and average cross sections

As neutron energy selection could not be realised for in-pile measurements, the obtained cross section values are averaged over the whole neutron energy distribution at the irradiation position. As a consequence, the cross sections in Eq. (6) are average cross sections and could not be simply replaced by the corresponding Maxwell-average cross sections but should be calculated on the basis of a modelised neutron flux:

$$< \sigma >= \frac{\int_0^\infty \sigma(E)\phi(E)dE}{\int_0^\infty \phi(E)dE} \tag{7}$$

where $\sigma(E)$ is the evaluated cross section as a function of the neutron energy given by data library and $\phi(E)$ the calculated neutron flux energy distribution. The latter quantity was calculated from a global, high statistics (5. 10^6 to 20. 10^6 generated neutrons from fission), simulation of the HFR core, reproducing properly the geometry and the fuel element history during the 50 days of reactor cycle, with MCNP code [12].

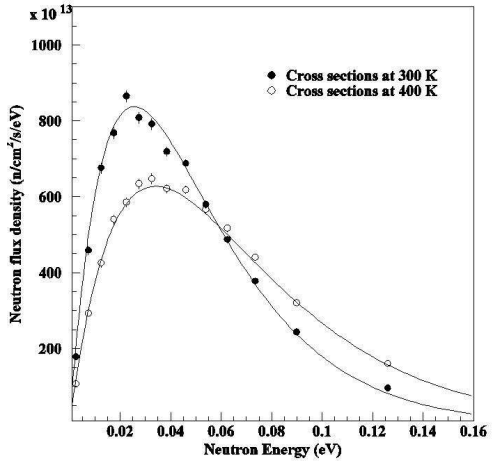

Fig. 1. Thermal component of the neutron flux in H9 calculated with MCNP (symbols) and cross section libraries prepared at 27^o C and 127^o C. Lines are Maxwellian distributions corresponding to temperatures fixed at 27^o C and 127^o C.

Neutron flux distributions have been calculated for different irradiation positions and for two moderator temperatures (27^o C and 127^o C) in order to frame the real temperature of the moderator which is of 50^o C. Results are

shown in Fig. 1 in the case of H9 where we clearly see Maxwellian distributions corresponding to temperature of 27^o C and 127^o C. The epithermal component is not visible on the figure but only about 2% of neutrons have energies greater than 1 eV. Thanks to the simple cylindrical geometry of the fuel element and the presence of D_2O moderator which has very well-known scattering cross sections, MCNP calculations are expected to give a good estimate of the real neutron energy distribution at 50 cm from the fuel element (irradiation position in H9 channel). This was validated in the V4 channel, which is closer from the fuel element than H9 channel, by dedicated cross-check experiments using fission micro-chambers and flux monitors [14].

Table 1
Ratios of averaged (calculated with Eq. (7)) and Maxwell-average cross sections ($\Lambda_{Max}(X)$), and averaged and point-like cross sections ($\Lambda_0(X)$). Also are indicated correction factors applied to the measured capture cross sections of ^{243}Am and ^{242}Pu in H9 (98% thermal spectrum at a temperature of 50^o C). $\Lambda_{Max}(Co) = 0.981$ and $\Lambda_0(Co) = 0.831$.

isotope X	$\Lambda_{Max}(X)$	$\Lambda_{Max}(Co)/\Lambda_{Max}(X)$	$\Lambda_0(X)$	$\Lambda_0(Co)/\Lambda_0(X)$
^{243}Am	1.057	0.928	0.905	0.918
^{242}Pu	1.178	0.833	1.000	0.831

In reference [11] an exhaustive analysis of the impact of the non-Maxwellian component of the neutron flux on the measurement of the thermal neutron cross sections, at different irradiation positions of the HFR, has been performed. Results for ^{243}Am and ^{242}Pu, in the case of irradiation in H9, are reported in Table 1. The study shows an agreement (at the level of a few percents) between averaged (as calculated with Eq. (7)) and Maxwell-average cross sections (the ratio is expressed as Λ_{Max} in Table 1), for a wide set of minor actinides, in the H9 irradiation position. However, for some actinides, as ^{242}Pu for instance, a huge resonance is close to the thermal energy region (see Fig. 2). For these isotopes, discrepancies can reach 20%, even for few percents of non-thermal neutrons.

In Table 1 is also reported the ratio Λ_0 between the averaged cross section calculated with Eq. (7) and the point-like cross section at 25 meV given by the data library used in the calculation. This quantity is used to derive experimental cross section at 25 meV from the measured one. The correction factor ($\Lambda_0(Co)/\Lambda_0(X)$) is then used in Eq. (6) to derive this value. By this method, the contribution of non-thermal neutrons is taken into account in the extraction of the point-like thermal neutron cross section, reducing by the way systematic errors due to the shape of the neutron flux distribution. An estimate of the errors associated to these correction factors shows that they do not exceed a few percents even for the most important ones.

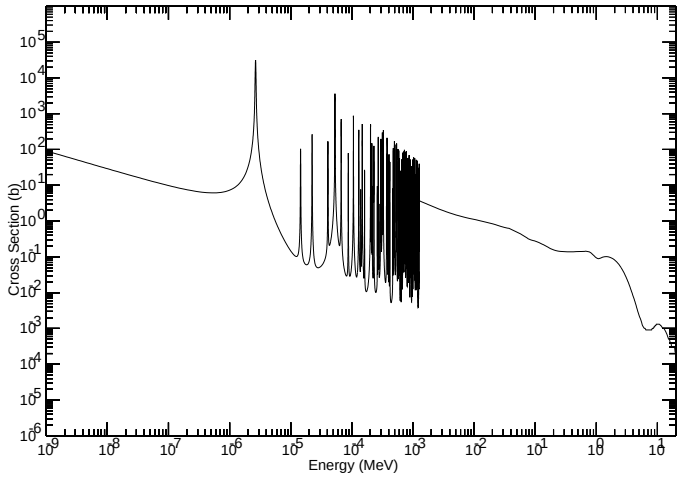

Fig. 2. ^{242}Pu neutron radiative capture cross section as a function of the neutron energy. Extracted from the ENDF-BVI data library [2].

Description of the Mini-INCA set-up

Irradiated samples are analysed by α- and γ-spectroscopy inside the "Mini-INCA" vacuum chamber [9] which is mechanically coupled to the H9 sample changer (see Fig. 3). The sample can move automatically from the irradiation position, inside the H9 beam tube, to a well defined position in front of the α and γ detectors (Fig. 5) with a repeatability precision better than 1%. This automatic control allows measurements of highly activated samples and a repetition of irradiations.

The sample is deposited onto a 4 μm nickel foil (Φ = 12 mm) surface by electrodeposition. The dimensions of the active deposit are limited to 5 mm in diameter. The thickness of the active layer is chosen to be thin enough to let the fission products, formed during the irradiation, and which could increase the gamma background, escape. The mass of the active deposit is chosen to be lower than 20 μg to limit the self-absorption of α-particles and the activity of the irradiated samples. The active target, together with a flux monitor foil, is placed inside a 0.4 mm thick titanium frame (see Fig. 4) in order to perform a simultaneous irradiation in the same neutron flux. The distance between the sample and the flux monitor is close to 2 cm that is smaller than spatial flux variations, as shown by irradiations of flux monitors placed on both side [9].

As shown in Fig. 5, the Mini-INCA chamber is equipped with two movable detectors placed on separate translation stages. The α-detector can move from 1 cm to 29.8 cm with respect to the sample position, and the γ-detector from 42.7 cm to 80.2 cm. As a consequence, the detection solid angles ($\Omega/4\pi$) range from 9. 10^{-5} to 6.4 10^{-2} and from 2.57 10^{-4} to 9.07 10^{-4}, respectively. By

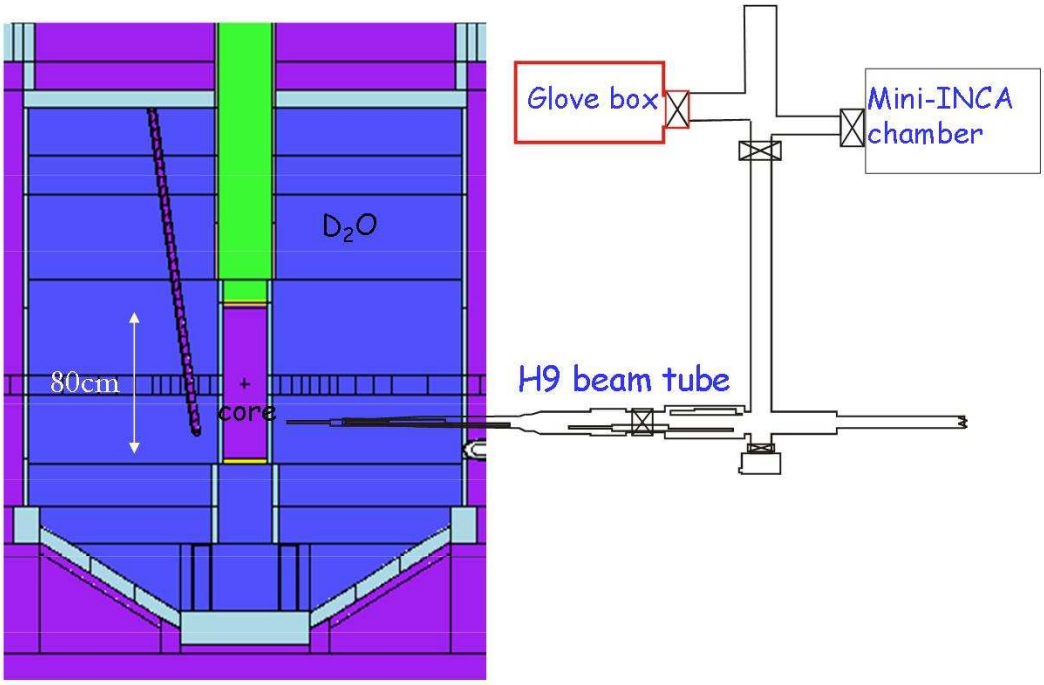

Fig. 3. Scheme of the implantation of the Mini-INCA chamber inside the ILL core reactor, and its connection to the H9 irradiation channel.

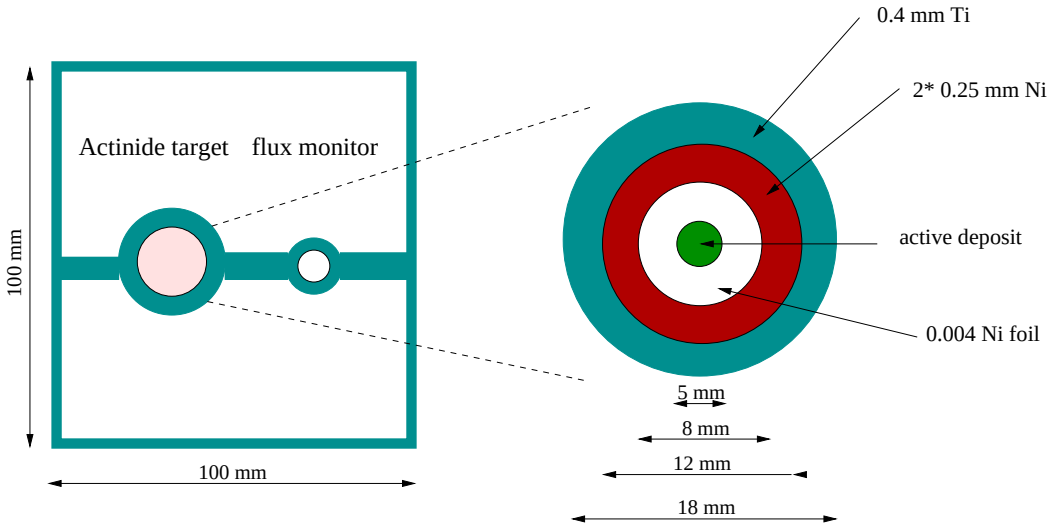

Fig. 4. Mini-INCA target holder (left) and active target (right).

adjusting the distance between the irradiated sample and the detectors it is then possible to find the most suitable counting rate. The apparatus is thus designed to measure very low activities (radioactive sample before irradiation, for instance) as well as high activities. The α-detector consists of a Passivated Implanted Planar Silicon (PIPS) [2] of 300 μm thick and 1.13 cm in diameter. A 3 mm Al plate collimator is placed in front of the sample to reduce the amount

[2] Canberra Industry

of β-particles produced by the decay of fission products in the detector. The typical detector resolution is 17 keV for ^{241}Am α-particle energies. The γ-detector is a high purity coaxial Germanium (GX1518[2]) of 4 cm thick and 5.15 cm in diameter, with a 500 μm carbon-epoxy entrance window. A 7 cm thick lead collimator is placed between the target and the detector to reduce the amount of γ-rays coming from the activated target holder frame. The typical resolution of the detector is 1.8 keV at 1.173 MeV. The electronic chain of the α-detector consists of a "classical" fast spectroscopy amplifier (model 2024[2]) whereas the electronic chain of the γ-detector includes a transistor reset preamplifier and a Digital Signal Processor module (DSP2060[2]). Special care for γ-spectroscopy was taken in order to allow accurate measurements even at high counting rates (up to $\sim$ 80 kHz) with a reasonable dead time. The acquisition dead time with pile-up rejection option is controlled at the level of 2% up to 60 kHz counting rates for the γ chain, and 15 kHz for the α chain. Both α and γ signals are acquired with a MPA acquisition module[3].

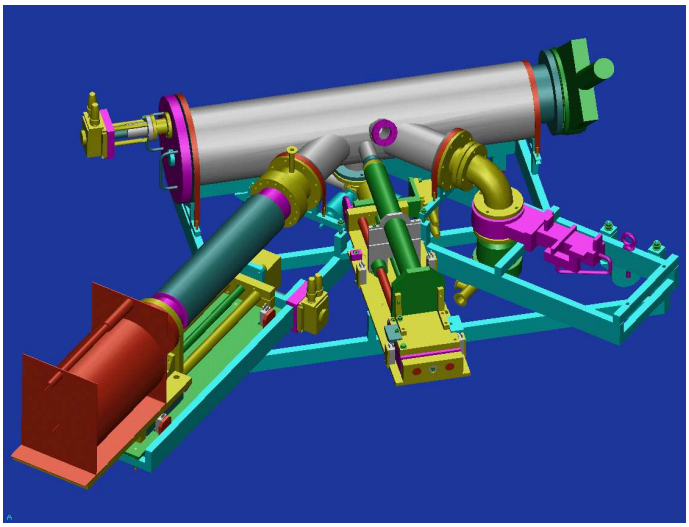

Fig. 5. Drawing of the Mini-INCA vacuum chamber where we can see the two movable trolleys supporting the γ-detector (left) and the α-detector (centre).

Detectors were calibrated in energy with standard α and γ sources. The Germanium detector photo-peak efficiency was determined experimentally with calibrated ($<$ 2% activity uncertainties) γ sources of ^{154}Eu, ^{241}Am and ^{60}Co [13]. For detector positions d ranging from 41.5 cm to 80 cm and γ energies E ranging from 26 keV to 1408 keV, detection efficiencies $\epsilon\Omega(E,d)$ have been fitted assuming:

$$\epsilon\Omega(E,d) = \epsilon(E) \times \Omega(E,d) = \epsilon(E) \times \omega(d) \times C(E,d) \qquad (8)$$

[3] MPA3 from FastComtec Industry

where $\omega(d)$ is point-like solid angle function normalized to 4π

$$\omega(d) = \frac{1}{2}\left(1 - \frac{1}{\sqrt{(\frac{\Phi^2}{4d^2} + 1)}}\right) \tag{9}$$

and $C(E, d)$ a correction factor to account from paralaxial effect. Measured efficiencies are connected together using the typical function (see Fig. 6):

$$\epsilon(E) = \exp\left(\sum_{i=1}^{6} a_i \ln(E)^{i-1}\right) \tag{10}$$

which gives, as an example, $\epsilon = 0.098 \pm 0.002$ at 1.17 MeV.

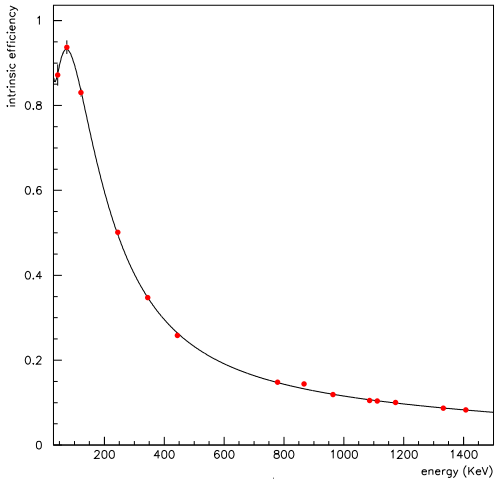

Fig. 6. Photo-peak efficiency of the Germanium detector at 80 cm as a function of the photon energy. Symbols are measurements with standard sources whereas the continuous line is an adjustement of the data with Eq. (10).

The solid angle equation (9) was also checked for α-detection system with 3% uncertainties ^{241}Am and ^{244}Cm standard α-sources and is checked for each measurements.

In order to reduce the background due to neutrons and gammas coming from the ILL reactor and to create a biological shielding, the Mini-INCA chamber is housed inside a casemate composed by a layer of B_4C blanket surrounded by a 5 cm thick borated polyethylene layer protected by a 5 cm thick lead layer.

Neutron flux measurement

The neutron fluency during the irradiation of ^{243}Am and ^{242}Pu samples was measured using a 6 mm diameter Al foil doped with 0.1% ^{59}Co, irradiated together with the actinide samples (see previous section and Fig. 4). The homogeneity of ^{59}Co inside the Al foil was certified to be 2% by the manufacturer [4] and the weighed masses of the monitors were (7.43±0.05) mg. The flux intensity was determined from Eq. (4), assuming a ^{59}Co neutron capture cross section averaged in the H9 flux of (31.1 ± 0.19) b [11,15], and found to be ϕ = 6.1 10^{14} $n/cm^2/s$ with a relative uncertainty of 3.8%, for both experiments.

$^{243}Am(n,\gamma)^{244}Am$ cross section determination

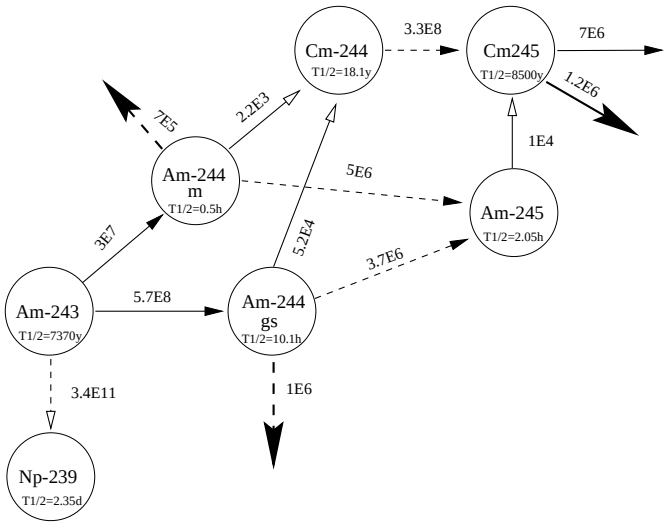

Fig. 7. Schematic view of the transmutation chain of ^{243}Am and produced isotopes. Numbers next to arrows indicate the characteristic time of reactions for a neutron flux intensity of 5. $10^{14} n/cm^2/s$.

As shown in Fig. 7, neutron capture on ^{243}Am leads to the production of short-lived ^{244}Am isotopes both of them decaying essentially to long-lived ^{244}Cm isotope. The $^{243}Am(n,\gamma)^{244gs+m}Am$ reaction cross section was measured via the α-decay of ^{244}Cm (two α-rays at 5804.8 and 5762.7 keV with intensities of (76.4 ± 0.2)% and (23.6 ± 0.2)%, respectively) after the complete decay of the two ^{244}Am states. We have irradiated 11.7 μg of pure ^{243}Am for 3

[4] Institut for Reference Materials and Measurements, Geel, Belgium

hours and 28 minutes in the H9 channel. The isotopic concentration of the initial sample was certified [4] and checked before the irradiation to be 99.987% of ^{243}Am, 0.002% of ^{242}Am and 0.011% of ^{241}Am. The irradiation time was chosen to produce enough ^{244}Cm isotope and to maintain the double capture on ^{244}Cm negligible. Moreover, the neutron flux was sufficiently low to neglect the fission and neutron-capture on both ^{244}Am states. A cooling time of at least 5 days was necessary before the measurement in order to let $^{244gs}Am$ decay into ^{244}Cm. By this time, the quantity of $^{244gs}Am$, the longer lifetime, was reduced by a factor of at least 4000.

An example of the obtained α-energy spectrum, measured at (19.83 ± 0.01) mm from the target, is shown in Fig. 8. Experimental data have been adjusted with a sum of empirical asymmetrical functions, common to all α-line energies. The asymmetrical function describes the shape of one α-particle taking into account the backscattered α at low energy and the degraded resolution due to pile-up events:

$$\begin{cases} F_r = & N\,(1-R_r)\,e^{-\frac{(E-E_0)^2}{2\sigma_r^2}} + R_r\,e^{-\frac{(E-E_0)}{\sigma_{r2}}} & \forall E > E_0 \\ F_l = & N\,(1-R_l)\,e^{-\frac{(E-E_0)^2}{2\sigma_l^2}} + \dfrac{R_l}{1+\left(\frac{(E_0-E)}{\sigma_{l2}}\right)^a} & \forall E < E_0 \end{cases} \tag{11}$$

where the "structural" parameters R_r, R_l, σ_l, σ_r, σ_{r2}, σ_{l2} and a are identical for all α-lines and depend only weakly on the counting rates. With this modelization and by summing over all the α-lines, the background due to other α-particles is properly estimated and we are able to obtain a global uncertainty of 2% on the net peak area.

The activities of ^{243}Am and ^{244}Cm were deduced from the adjustement of the measured α-line intensities at different distances from the target with the solid angle Eq. (9). Using Eq. (4), we obtained a value of

$$< \sigma_c^{gs+m}(^{243}Am) >= 74.1 \pm 3.3\ b$$

for the $^{243}Am(n,\gamma)^{244gs+m}Am$ averaged thermal neutron capture cross section. The σ_0^{gs+m} value at 0.025 eV was extracted from the above value using the correction factor listed in Table 1 to account for the non-thermal part of the neutron spectrum. The obtained value is:

$$\sigma_0^{gs+m} = 81.8 \pm 3.6\ b$$

In Table 2, the new value for the $\sigma_c^{gs+m}(^{243}Am)$ is compared with values coming from previous experiments and evaluated data libraries. It is clear that large

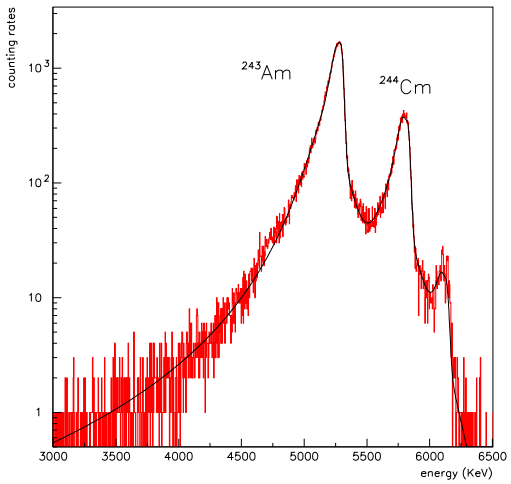

Fig. 8. α-energy spectrum of irradiated ^{243}Am sample obtained after 6 days of cooling. Data have been adjusted with a sum of asymmetrical functions for each α-ray as described in the text.

Table 2
Comparison of the measured $^{243}Am(n,\gamma)^{244gs+m}Am$ capture cross section in this work with existing experimental and evaluated data.

$\sigma_c^{gs+m}(^{243}Am)$	Method	Year	Reference
81.8 ± 3.6 b	Activation + Spectroscopy	2005	This work
84.4 b	Activation + Spectroscopy	1997	[16]
83 ± 6 b	Activation + Spectroscopy	1975	[17]
73.6 ± 1.8 b	Activation + Spectroscopy	1957	[18]
78.0 b	Radiochemistry	1968	[19]
$66 < \sigma < 84$ b	Activation + Spectroscopy	1966	[27]
140 ± 50 b	Activation + Spectroscopy	1954	[20]
115 b	Radiochemistry	1954	[21]
75.10 b	ENDFB-VI.8		[2]
76.75 b	JENDL3.3		[3]
76.72 b	JEFF3.1		[1]

discrepancies exist between the older and the most recent experiments. The value proposed in this work is 9% higher than the adopted values in the data libraries but compatible with the most recent experiments [16,17] which reported values of (84.4) and (83 ± 6) b.

The partial $^{243}Am(n,\gamma)^{244gs}Am$ cross section was measured within the previous experiment, via the γ-decay of $^{244gs}Am$ (two γ-rays, one at 744 keV with an intensity of $(66 \pm 18)\%$ and the other at 898 keV with an intensity of $(28 \pm 8)\%$) after 40 hours of cooling time. Due to the high activity inside the detector (2 MHz just after the irradiation), saturating the electronic, measurements were not feasible before this time. Even after 40 hours the dead time of the electronic was still of about 50%, which is close to the limit of the DSP. The high activity was essentially caused by short lived isotopes contained in the target holder: Ti, Ni and Mn, and a contaminant: ^{198}Au. In these conditions, the γ-decay of ^{244m}Am, with its short half-live of 26 minutes, was not visible and thus the $^{243}Am(n,\gamma)^{244m}Am$ cross section was not measurable. A dedicated experiment using specific electronic developed to stand very high counting rates is foreseen to measure this cross section.

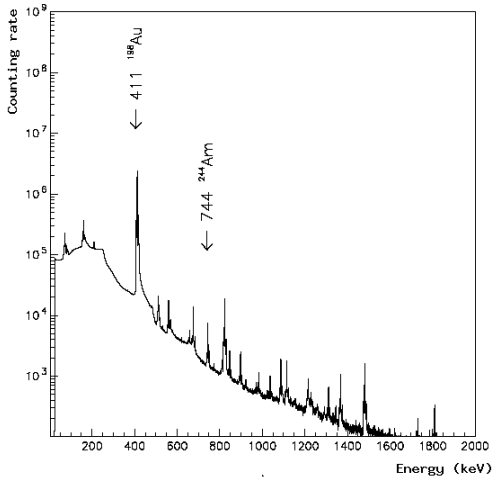

Fig. 9. The ^{243}Am γ-spectrum after 40 hours of cooling time. The most intense $^{244gs}Am$ γ-line is indicated together with the contaminant which contributes the most to the global activity of the sample: ^{198}Au.

The γ-energy spectrum is shown in Fig. 9 where we see the gamma lines of $^{244gs}Am$ and ^{198}Au (the most significant contributing contaminant to the global activity). The analysis of the γ-ray spectra was done by fitting the γ-photopeak with a Gaussian function added to a linear background. The activity was measured as a function of time and corrected for the decay. A mean activity of (1.74 ± 0.52) 10^7 Bq was deduced from the measurements performed between 40 and 60 hours of cooling time.

With the same procedure as described before, we found an averaged capture

cross section value of:

$$< \sigma_c^{gs}(^{243}Am) >= 4.7 \pm 1.4\ b$$

and a thermal neutron capture cross section at 0.025 eV of:

$$\sigma_0^{gs} = 5.2 \pm 1.56\ b$$

The error bars are essentially dominated by the error associated to the γ-ray intensity used to measure the amount of $^{244gs}Am$ by the end of irradiation. Nevertheless, it provides a new value for $^{243}Am(n,\gamma)^{244gs}Am$ reaction which falls within the range of existing data, 3.9 to 5.9 b [27,22]. Another dedicated experiment at ILL is planned to improve the accuracy on this value.

$^{242}Pu(n,\gamma)^{243}Pu$ cross section

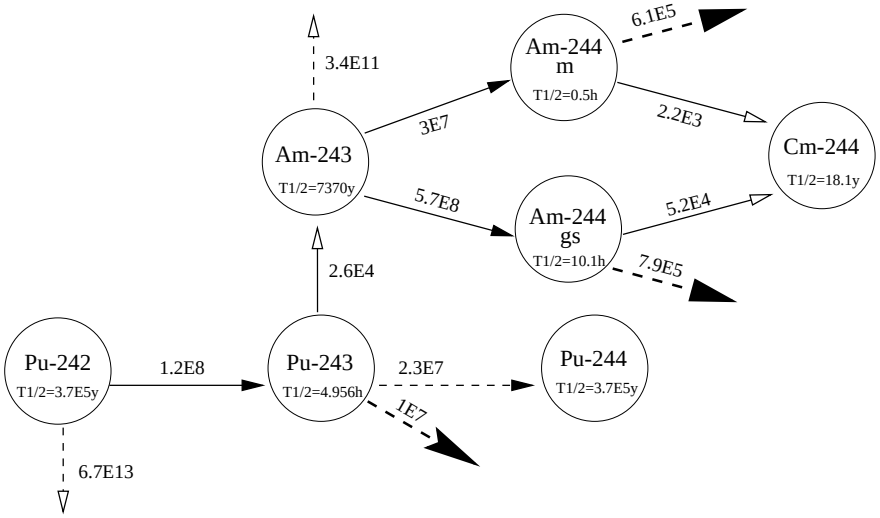

Fig. 10. Schematic view of the transmutation chain of ^{242}Pu. Numbers next to arrows indicate the characteristic time of reactions for a neutron flux intensity of 5. $10^{14} n/cm^2/s$.

As for the previous reaction study, the $^{242}Pu(n,\gamma)^{243}Pu$ cross section was measured via the α-decay of ^{243}Am formed after the complete decay of ^{243}Pu [5].

We have irradiated 10.5 μg of ^{242}Pu for 2 days. The isotopic composition was certified [4] and checked before irradiation to be: 99.932% of ^{242}Pu, 0.004% of ^{238}Pu, 0.005% of ^{239}Pu, 0.022% of ^{240}Pu, 0.035% of ^{241}Pu and 0.002% of

[5] Due to a high γ-background, the measurement of the 84 keV line associated with the β decay of ^{243}Pu and 74.7 keV line associated with the α decay of ^{243}Am, was not possible

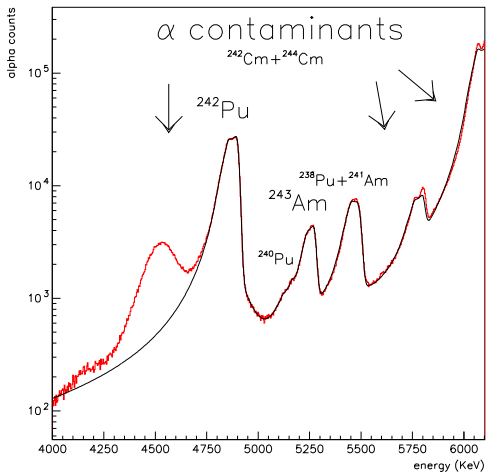

Fig. 11. α-spectrum of ^{242}Pu sample after 2 days of irradiation. Note the broad α-peak at low energy corresponding to contaminants deposited on the back side of the target layer.

Table 3
Comparison of the measured $^{242}Pu(n,\gamma)^{243}Pu$ cross section in this work with existing experimental and evaluated data.

$\sigma_c(^{242}Pu)$	Method	year	Reference
22.5. $\pm$ 1.1 b	Activation + Spectroscopy	2005	This work
18.7 $\pm$ 0.7 b	Activation + Spectroscopy	1970	[23]
18.5 $\pm$ 1 b	Prompt γ-Spectroscopy	1979	[24]
18.6 $\pm$ 0.8 b	Activation + Spectroscopy	1956	[25]
30 $\pm$ 10 b	Radiochemistry	1956	[26]
18 $< \sigma <$ 23 b	Radiochemistry	1966	[27]
19.16 b	ENDFB-VI.8		[2]
18.76 b	JENDL 3.3		[3]
18.79 b	JEFF 3.1		[1]

^{244}Pu. An example of recorded α-spectrum is shown in Fig. 11. Using the same data analysis technique that described before, we found an averaged capture cross section value of:

$$< \sigma_c(^{242}Pu) >= 22.5 \pm 1.1\ b$$

and we deduced a thermal neutron capture cross section value at 0.025 eV of:

$$\sigma_0 = 22.5 \pm 1.1\ b$$

As previously, the value obtained in this work is compared with existing data in Table 3. This value is 18% higher than previous experiment values and than the library values. Only two over six experiments performed between 1954 and 1979 give compatible values [26,27] but with very large error bars. The correction with respect to a "theoretical" $\frac{1}{v}$ behavior of the cross section at thermal energy is important (17%) as already mentioned previously, and could explain the discrepancies with older measurements for which the neutron flux distribution was less better characterized than in our experiments.

Conclusions

New measurements of ^{243}Am and ^{242}Pu capture cross sections at thermal energies have been performed using the new α and γ-spectroscopy station of the Mini-INCA project at the ILL reactor. Thanks to the intense and quasi-pure thermal neutron flux available in H9, thermal neutron cross section have been extracted with a minimum of corrections. The new results show some discrepancies with evaluated libraries and with older measurements but are in good agreement with the recent ones. These accurate measurements provide a new set of data for two important minor actinides responsible, in part, for the long term radio-toxicity of nuclear wastes. In the near future, the experiment on ^{243}Am will be repeated with a new electronic specifically designed for very high counting rates to determine the $^{243}Am(n,\gamma)^{244m}Am$ cross section and improve the accuracy on the $^{243}Am(n,\gamma)^{244gs}Am$ cross section determination. In the future, the experimental program will be extended to other minor actinides of interest [7] (^{237}Np, ^{243}Cm, ...) to improve the reliability of nuclear data that are necessary for the study of the optimal incineration conditions for the next generation systems dedicated to the transmutation of nuclear wastes.

Acknowledgments

We would like to thank the ILL direction and the ILL reactor division for their support and help all along the elaboration of the Mini-INCA project. A special thanks also to the DSM/DAPNIA/SIS for the realization and the technical development of the Mini-INCA project.

References

[1] JEFF-3.3 http://www.nea.fr/html/dbdata/JEFF.

[2] ENDF/B-VI.8 http://www.nndc.bnl.gov/exfor/endf00.htm.

[3] JENDL-3.3 http://wwwndc.tokai.jaeri.go.jp/jendl/j33/j33.html.

[4] F. Storrer and A. Zaetta, Internal Report CEA/DEN/DER/SPRC/LECy 2001-301 (2001).

[5] G.Fioni, M. Cribier, F. Marie et al, Nucl. Phys., A 693, 546 (2001).

[6] F. Marie et al., Internal Report, DAPNIA/SPhN-00- CSTS (16 dec 2002).

[7] F. Marie et al., Internal Report, DAPNIA/SphN-00-50 (2000).

[8] M. Benedict, T.H. Pigford and H.W. Levi, Nuclear Chemical Engineering, Mc Graw Hill, New York (1985).

[9] O. Déruelle, PhD Thesis, Université d'Orsay - Paris XI, DAPNIA-02-06-T (2002) (in French).

[10] A. Letourneau et al., Proceedings of International Conference on Nuclear Data for Science and Technology, 26 Sept.- 1 Oct., Santa Fe, USA (2004).

[11] A. Letourneau, F. Marie, D. Ridikas, Internal report, DAPNIA-03-243 (2003).

[12] D. Ridikas et al., Proceedings of the 5^{th} Int. Specialist's Meeting SATIF-5, OECD/NEA,- Paris, 383 (2000).

[13] O. Déruelle, F. Marie et al., Proceedings of the 11th International Symposium on Capture Gamma-Ray Spectroscopy and Related Topics, 2-6 september, Prague, Czech Republic (2002).

[14] M. Fadil, PhD Thesis, INPG - Grenoble, DAPNIA-03-01-T (2003).

[15] R.B. Firestone et al, Table of Isotopes, Virginia Shirley editor 8^{th} ed.

[16] Y. Hatsukawa et al., JAERI Tokai report series, 98-003, 221 (1997).

[17] V.D. Gravilov et al, Atomnaya Energiya, 41, 185 (1975).

[18] J.P. Butler et al., Can. Jour. of Physics, 35, 147 (1957).

[19] R.L. Folger et al., Nuclear Cross-Sections Techn. Conf., Washington, 2 (1968).

[20] B.G. Harvey et al., Phys. Rev., 95, 581 (1954).

[21] C. M.Stevens et al., Phys. Rev., 94, 974 (1954).

[22] R.P. Schuman et al, Idaho Nuclear Corp, Report IN-1126,19 (1967)

[23] R.W. Durham et F.Molson, Can. Jour. of Physics, 48,716 (1970).

[24] P.J. Bendt et E.T.Jurney, Los Alamos Scientific Lab. Reports, 7853, (1979).

[25] J. Butler et al., Can. Journal of Chemistry, 34, 253, (1956).

[26] P.R. Fields et al., Nucl. Science and Engineering, 1, 62, (1956).

[27] C.H. Ice, Savannah River Reports, MS-66, 69, (1966).